

Nature versus nurture: what regulates star formation in satellite galaxies?

Gabriella De Lucia^{1*}, Michaela Hirschmann², Fabio Fontanot¹

¹*INAF - Astronomical Observatory of Trieste, via G.B. Tiepolo 11, I-34143 Trieste, Italy*

²*UPMC-CNRS, UMR7095, Institut d’Astrophysique de Paris, F-75014 Paris, France*

Accepted ????. Received ??? in original form ???

ABSTRACT

We use our state-of-the-art Galaxy Evolution and Assembly (GAEA) semi-analytic model to study how and on which time-scales star formation is suppressed in satellite galaxies. Our fiducial stellar feedback model, implementing strong stellar driven outflows, reproduces relatively well the variations of passive fractions as a function of galaxy stellar mass and halo mass measured in the local Universe, as well as the ‘quenching’ time-scales inferred from the data. We show that the same level of agreement can be obtained by using an alternative stellar feedback scheme featuring lower ejection rates at high redshift, and modifying the treatment for hot gas stripping. This scheme over-predicts the number densities of low to intermediate mass galaxies. In addition, a good agreement with the observed passive fractions can be obtained only by assuming that cooling can continue on satellites, at the rate predicted considering halo properties at infall, even after their parent dark matter substructure is stripped below the resolution of the simulation. For our fiducial model, the better agreement with the observed passive fractions can be ascribed to: (i) a larger cold gas fraction of satellites at the time of accretion, and (ii) a lower rate of gas reheating by supernovae explosions and stellar winds with respect to previous versions of our model. Our results suggest that the abundance of passive galaxies with stellar mass larger than $\sim 10^{10} M_{\odot}$ is primarily determined by the self-regulation between star formation and stellar feedback, with environmental processes playing a more marginal role.

Key words: galaxies: evolution - galaxies: formation

1 INTRODUCTION

It has long been known that the physical properties of galaxies exhibit strong correlations with the environment they live in. Galaxies in over-dense regions have typically more evolved (elliptical) morphologies, lower gas masses, redder colours, and lower star formation rates than galaxies of similar mass living in regions of the Universe with mean density (e.g. Oemler 1974; Dressler 1980; Giovanelli & Haynes 1983). In more recent years, studies on the subject have received much impetus from the completion of large spectroscopic surveys both in the local Universe and at higher redshift (Kauffmann et al. 2004; Balogh et al. 2004; Cooper et al. 2012; Fossati et al. 2017; Cucciati et al. 2017, just to name a few).

At $z=0$, a detailed characterization of the role of environment on the physical properties of galaxies has been obtained using group/cluster catalogues based on data from the Sloan Digital Sky Survey (SDSS). These stud-

ies have shown that the fraction of red/passive galaxies increases with increasing galaxy stellar mass, parent halo mass, and local density, and that the colour/star formation activity distribution is bimodal across all range of halo masses/environments probed (e.g. Weinmann et al. 2006a; Baldry et al. 2006; Kimm et al. 2009; Peng et al. 2010; De Lucia et al. 2012; Wetzel et al. 2012; Hirschmann et al. 2014). These observations are often interpreted in a ‘satellite versus centrals framework’: galaxies located at the centre of the dominant halo are defined as ‘central’ galaxies, while the others are classified as ‘satellites’. While this scheme is intuitive and straightforward from the theoretical point of view, its application to observational data is generally more difficult and typically requires mock simulated catalogues for calibration¹. Adopting this interpretative scheme, observational measurements in the local Universe have been used to constrain the efficiency and time-

¹ For a discussion about the applicability of the framework, and about its general relevance in studies of galaxy evolution, we refer to De Lucia, Muzzin & Weinmann (2014a)

* E-mail: gabriella.delucia@inaf.it

scales of physical processes affecting the star formation activity of satellite galaxies. [De Lucia et al. \(2012\)](#) combined galaxy merger trees extracted from semi-analytic models with measurements of the red/passive fractions of satellites in groups/clusters, and estimated quenching time-scales varying between 5 and 7 Gyr. [Wetzel et al. \(2013\)](#) constrained satellite star formation histories combining infall histories extracted from high-resolution N-body simulations with measurements of the specific star formation rate (i.e. the ratio between the star formation rate and the galaxy stellar mass, $\text{SFR}/M_{\text{star}}$) distribution. They put forward a so called ‘delayed-then-rapid quenching’ scenario for satellite galaxies: the specific SFRs are unaffected for 2-4 Gyr after infall, and then decay on a very short time-scale (e-folding time < 0.8 Gyr). [Hirschmann et al. \(2014\)](#) revisited the analysis by [De Lucia et al. \(2012\)](#) extending it to the dependence of the quiescent fraction on local galaxy density, and demonstrated that the inferred long quenching time-scales were difficult to achieve in the framework of the back then state-of-the-art semi-analytic models. The studies just mentioned all focused on galaxies with stellar mass larger than $\sim 10^{9.5} M_{\odot}$. At lower galaxy stellar masses ($< 10^8 M_{\odot}$) the quenching efficiency appears to increase dramatically, possibly as a consequence of the increasing importance of ram-pressure stripping ([Fillingham et al. 2015, 2016](#)).

From a theoretical standpoint, central galaxies occupy a ‘special’ location where cold gas accretion can take place either rapidly along filamentary structures at high redshift, or more gradually, cooling from a quasi-static hot atmosphere, at low redshift and in more massive haloes. When a galaxy is accreted onto a larger system (i.e. it becomes a satellite), its hot gas reservoir is typically assumed to be instantaneously and completely removed, so that no new replenishment of the cold gas is possible through gas cooling. This process is usually referred to as ‘strangulation’ or ‘starvation’, and simulation studies have argued that a non negligible amount of hot gas can remain in place even several Gyrs after accretion ([McCarthy et al. 2008](#)). In addition, a number of different physical processes can effectively reduce the cold gas content of satellite galaxies. For example, satellite galaxies travelling at high velocities through a dense intra-cluster medium suffer a strong ram-pressure stripping that can sweep cold gas out of the stellar discs ([Gunn & Gott 1972](#)). Repeated high-speed encounters with other satellite galaxies ([Farouki & Shapiro 1981; Moore et al. 1996](#)) and, more generally, galaxy-galaxy interactions (e.g. [Mihos 2004](#)) can lead to a strong internal dynamical response, triggering the conversion of part of the available cold gas into stars. In modern theoretical models of galaxy formation, these physical processes are typically combined with efficient stellar feedback schemes, which translates in a rather rapid depletion of the cold gas reservoir associated with satellite galaxies, and an excess of red/passive galaxies with respect to the observations (e.g. [Weinmann et al. 2006b; Wang et al. 2007](#)).

When this problem was first noted, about one decade ago, the attention of the community focused on the ‘simplified’ treatment of satellite galaxies and, in particular, on the assumption that the hot gas reservoir is instantaneously stripped at the accretion time. In later studies, based on semi-analytic models, a more gradual stripping of the hot gas has been assumed. Albeit improved, how-

ever, the agreement with observational measurements has been far from satisfactory (e.g. [Kang & van den Bosch 2008; Font et al. 2008; Weinmann et al. 2010; Guo et al. 2011; Hirschmann et al. 2014](#)). The problem has not been limited to semi-analytic models ([Weinmann et al. 2012](#)), and it still appears in state-of-the-art hydrodynamical simulations. For example, in the Hydrangea simulations ([Bahé et al. 2017](#)), that adopt the galaxy formation model developed for the EAGLE project, the fraction of passive satellites *decreases* with increasing stellar mass, which is opposite to what is observed. In addition, the fraction of passive satellites predicted by these simulations is significantly larger than observed for intermediate to low mass satellites (see Fig. 6 in [Bahé et al. 2017](#)). A comparison with predictions from the Illustris simulation was published in [Sales et al. \(2015\)](#), who analysed the projected radial distribution of satellites split by colour, and found a good agreement with observational measurements based on SDSS. The agreement was ascribed to the large (relative to earlier work) gas contents of satellite galaxies at the time of infall. In fact, [Sales et al. \(2015\)](#) show (see their Fig. 3) that the gas fractions of infalling satellites in Illustris are significantly larger than those predicted by the semi-analytic model by [Guo et al. \(2011\)](#), and in quite good agreement with local observations of HI in galaxies. While it would be useful to see a more detailed comparison between these simulations (as well as their next generation - [Pillepich et al. 2018](#)) and the measured variations of passive fractions as a function of halo and galaxy mass, the nature of the simulations makes it difficult (and certainly computationally very expensive) to understand exactly *why* (i.e. through which physical processes) a better agreement with observational results can be achieved. The flexibility of the semi-analytic approach is an advantage in this case, as it allows us to disentangle efficiently the relative importance of different processes using large simulated volumes.

A few recent renditions of semi-analytic models exhibit a relatively good agreement with observational data. Contrary to what was originally expected, the success of these models is not driven by an improved satellite treatment: [Hirschmann et al. \(2016\)](#) have shown that the predicted variations of passive fractions as a function of galaxy stellar mass are sensitive to the adopted stellar feedback scheme. In addition, they have been able to identify schemes that reproduce well the observational measurements, albeit adopting an instantaneous stripping of the hot gas reservoir at infall. [Henriques et al. \(2017\)](#) have used a different approach: they have re-tuned the parameters of their galaxy formation model to explicitly fit the measured fractions of passive galaxies. This process required important modifications for both their star formation and stellar feedback schemes, in addition to modifying the treatment of hot gas stripping.

In this paper, we will use our state-of-the-art GALaxy Evolution and Assembly (GAEA) semi-analytic model to analyse in detail the time-scales over which star formation in satellite galaxies is suppressed, and their dependence on different physical treatments. The layout of the paper is as follows: in Sections 2, we will introduce the model runs used in this study. In Section 3, we will compare model predictions with the distributions of specific SFRs and variations of passive fractions as a function of galaxy stellar mass and halo mass, as measured in the local Universe. In Section 4, we will quantify the time-scales over which the star formation

in present-day satellite galaxies is suppressed in our models. In Section 5 we discuss our results, and compare model predictions with estimates of passive fractions and quenching time-scales at earlier cosmic times. Finally, in Section 6, we give our conclusions.

2 THE GAEA GALAXY FORMATION MODEL

The GAEA semi-analytic model builds on the model published in De Lucia & Blaizot (2007), but many prescriptions have been updated significantly over the past years. In particular, the model features a sophisticated chemical enrichment scheme that accounts for the non-instantaneous recycling of gas, metals and energy (De Lucia et al. 2014b), and a modified stellar feedback scheme that is partly based on results from numerical simulations (Hirschmann et al. 2016).

Specifically, we assume that the reheating rate of cold disk gas, due to supernovae explosions and winds from massive stars, can be parametrized using the fitting formulae provided by Muratov et al. (2015). These are based on the FIRE (Feedback In Realistic Environments) set of hydrodynamical simulations (Hopkins et al. 2014). We also assume that the same parametrizations can be adopted to model the rate of energy injection in the inter-stellar medium, and model the gas ejection rate outside galactic haloes following energy conservation arguments as in Guo et al. (2011). Finally, we assume that ejected gas can be re-accreted onto the hot gas component associated with central galaxies on a time-scale that depends on halo mass, as in Henriques et al. (2013). For a detailed description of the modelling adopted for stellar feedback (HDLF16-FIRE hereafter), we refer to Hirschmann et al. (2016). In previous work, we have shown that, in our GAEA framework, this feedback scheme allows us to reproduce nicely the fraction of passive galaxies measured in the local Universe, and its variation as a function of galaxy stellar mass, both for central and satellite galaxies. In addition, we have also shown that the HDLF16-FIRE feedback scheme reproduces the observed evolution of the galaxy stellar mass function and the cosmic star formation rate up to $z \sim 10$, as well as a number of other important observational constraints (Hirschmann et al. 2016; Fontanot et al. 2017; Zoldan et al. 2017; Xie et al. 2017; Zoldan et al. 2018).

In the following sections, we will compare predictions from our fiducial model with those from a run adopting the ‘energy-driven’ feedback scheme used in De Lucia et al. (2004) and De Lucia et al. (2014b). This model (hereafter HDLF16-ED) assumes that: (i) the reheating rate is proportional to the inverse of the square virial velocity; (ii) all gas reheated in central galaxies is ejected, while gas reheated in satellites is added to the hot gas reservoir associated with centrals; and (iii) ejected gas is re-incorporated on a halo dynamical time-scale (see first row of Table 1 in Hirschmann et al. 2016). The HDLF16-ED feedback has been adopted in previous versions of our model, and is meant to illustrate how much model predictions can vary depending on the assumed stellar feedback scheme.

Both the HDLF16-FIRE and the HDLF16-ED runs assume that the hot gas halo associated with infalling galaxies is instantaneously stripped at the time these are accreted onto larger systems. As discussed above, this assumption has important consequences on the evolution of satellite galaxies.

In order to quantify how much the star formation history of satellites can be affected by a different treatment for hot gas stripping, we also consider two alternative runs. These (ED-NOSTR1 and ED-NOSTR2) adopt the HDLF16-ED feedback scheme, but relax the instantaneous stripping assumption. Specifically, satellite galaxies are able to retain their hot gas halo, which then replenishes the cold disk gas via gas cooling. We also assume that the cooling rate on satellite galaxies can be reduced (and eventually balanced) by radio mode feedback from Active Galactic Nuclei (AGN). For these two physical processes, we adopt the prescriptions detailed in De Lucia et al. (2010) and Croton (2006), respectively. We evolve satellite galaxies using the properties of their parent substructures at the time of infall (i.e. at the last time these were central haloes). When subhalos are stripped below the resolution limit of the simulation, our model assumes that the hosted galaxies survive as ‘orphans’, and merge with the corresponding central galaxies after a residual merging time based on the Chandrasekar approximation (see De Lucia & Blaizot 2007 and De Lucia et al. 2010 for details). In the ED-NOSTR1 run, we assume that the residual hot gas associated with orphan galaxies is stripped and added to the hot gas reservoir of the parent halo. In an alternative run (hereafter ED-NOSTR2), we assume that cooling can take place also on orphan galaxies, until the hot gas reservoir is exhausted, or the galaxy merges. This is clearly unrealistic, as a significant stripping of the parent subhalo is bound to lead to some stripping of the baryonic component of the hosted galaxy (unless subhalo stripping is exclusively numerical). Therefore, this run provides a lower limit to the fraction of passive satellites that can be obtained by only modifying the treatment of hot gas stripping, in the framework of our HDLF16-ED model. In all runs considered, the gas ejected from satellite galaxies is associated with the ejected reservoir associated with the corresponding central galaxy. Finally, it is worth stressing that, with the exception of the HDLF16-FIRE run, all model variations considered (including the HDLF16-ED run) do not reproduce the measured evolution of the galaxy stellar mass function.

All model predictions shown in the following are based on merger trees extracted from the Millennium Simulation (Springel et al. 2005). This is a pure dark matter N -body simulation of a box of 500 Mpc h^{-1} on a side, assuming cosmological parameters consistent with WMAP1 ($\Omega_\Lambda = 0.75$, $\Omega_m = 0.25$, $\Omega_b = 0.045$, $n = 1$, $\sigma_8 = 0.9$, and $H_0 = 73 \text{ km s}^{-1} \text{ Mpc}^{-1}$). Although these cosmological parameters are now out-to-date (more recent measurements favour in particular a lower value for σ_8), previous work has shown that model results are qualitatively unaffected by relatively small variations of their values, once the physical parameters of the model are re-tuned to reproduce a given set of observational results in the local Universe (Wang et al. 2008; Guo et al. 2013). All figures presented below have been constructed analysing about 20 per cent of the volume of the simulation, but we have verified that results do not vary significantly when considering a larger volume.

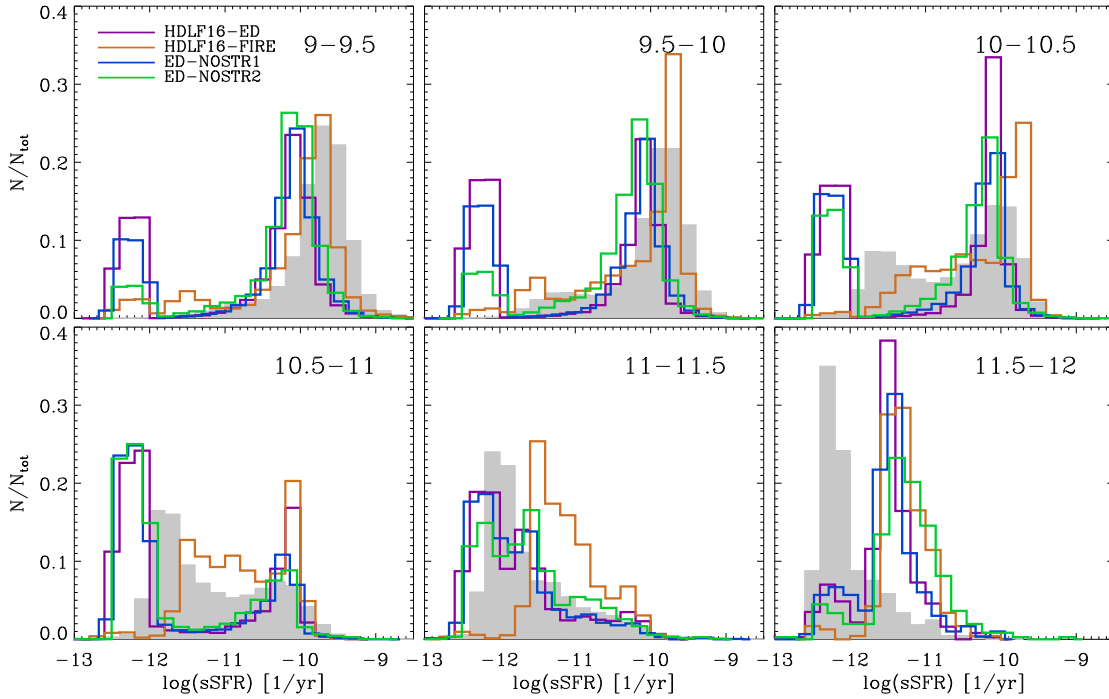


Figure 1. Distributions of specific SFRs for different stellar mass bins (different panels) at $z = 0$, as predicted by the different feedback/satellite models considered in this study (HDLF16-ED: lila; HDLF16-FIRE: orange; ED-NOSTR1: green; ED-NOSTR2: red). Model predictions are compared with observational data from SDSS, shown by the gray histograms.

3 PASSIVE GALAXY FRACTIONS IN THE LOCAL UNIVERSE

Fig. 1 shows the distributions of specific SFRs for different galaxy stellar mass bins (different panels, as indicated in the legend). Lines of different colours correspond to the different runs introduced above, while gray histograms show observational estimates from [Hirschmann et al. \(2014\)](#). These are based on data from the SDSS DR8, cross-correlated with the JHU-MPA DR7 catalogue² and the updated DR7 version of the group catalogue by [Yang et al. \(2007\)](#). The specific SFRs shown are based on measurements published in [Brinchmann et al. \(2004\)](#), with modifications regarding the treatment of dust attenuation and aperture corrections as described in [Salim \(2007\)](#). Only model galaxies brighter than -18 in the r -band have been considered, as in the observational sample. Model galaxies with zero SFR³ are included by assuming specific SFR values following a Gaussian distribution centred at 12.5 yr^{-1} , with a dispersion of 0.25 yr^{-1} .

None of the models considered here reproduces well the observed distributions. For the lowest mass bin considered, the HDLF16-FIRE run over-predicts slightly the number of passive galaxies, but extends to specific SFR values larger than those predicted by the other three runs, and is in better agreement with the peak corresponding to ‘active’ galaxies in the observed distribution. For the same stellar mass bin,

the HDLF16-ED run and its variants over-predict significantly the fraction of passive galaxies, and active galaxies peak at a value that is offset low with respect to the observational measurements. At intermediate galaxy stellar masses, the HDLF16-ED run and its variants over-predict the numbers of passive galaxies, but exhibit a clearly bimodal distribution as in the observational data. The HDLF16-FIRE run performs better in terms of passive fractions, but the distribution is less bimodal and the passive peak is moved to higher values of specific SFR with respect to the observations. For the most massive bin considered, all model distributions are offset towards larger values of specific SFR with respect to the observed distribution, i.e. model galaxies tend to be more active than observed. In [Hirschmann et al. \(2016\)](#), we ascribed this failure to the adopted scheme for AGN feedback. We have not been able, however, to improve the agreement with observational data via a simple modification of the efficiency of this form of feedback, which suggests the problem might have a more complex origin and solution.

In the following analysis, following [Hirschmann et al. \(2016\)](#), we select as passive galaxies all those with specific SFR smaller than $0.3 \times t_{\text{Hubble}}^{-1} \approx 10^{-11} \text{ yr}^{-1}$ (see also [Franx et al. 2008](#)). The model distributions shown in Fig. 1 are not in agreement with observational estimates, but are such that the adopted threshold assures that the predicted passive fractions are not very sensitive to this mismatch.

Fig. 2 shows the fraction of passive galaxies as a function of galaxy stellar mass (left column) and parent halo mass (right column), as predicted by all model runs considered (lines of different colours), and as estimated from data (symbols with error bars). Different rows show results for all galaxies (top), centrals only (middle), and satellites (bot-

² <http://www.mpa-garching.mpg.de/SDSS/DR7/>

³ The distributions shown here for the runs HDLF16-FIRE and HDLF16-ED differ from those shown in Fig. 8 of [Hirschmann et al. \(2016\)](#) because galaxies with zero SFR were excluded in that work.

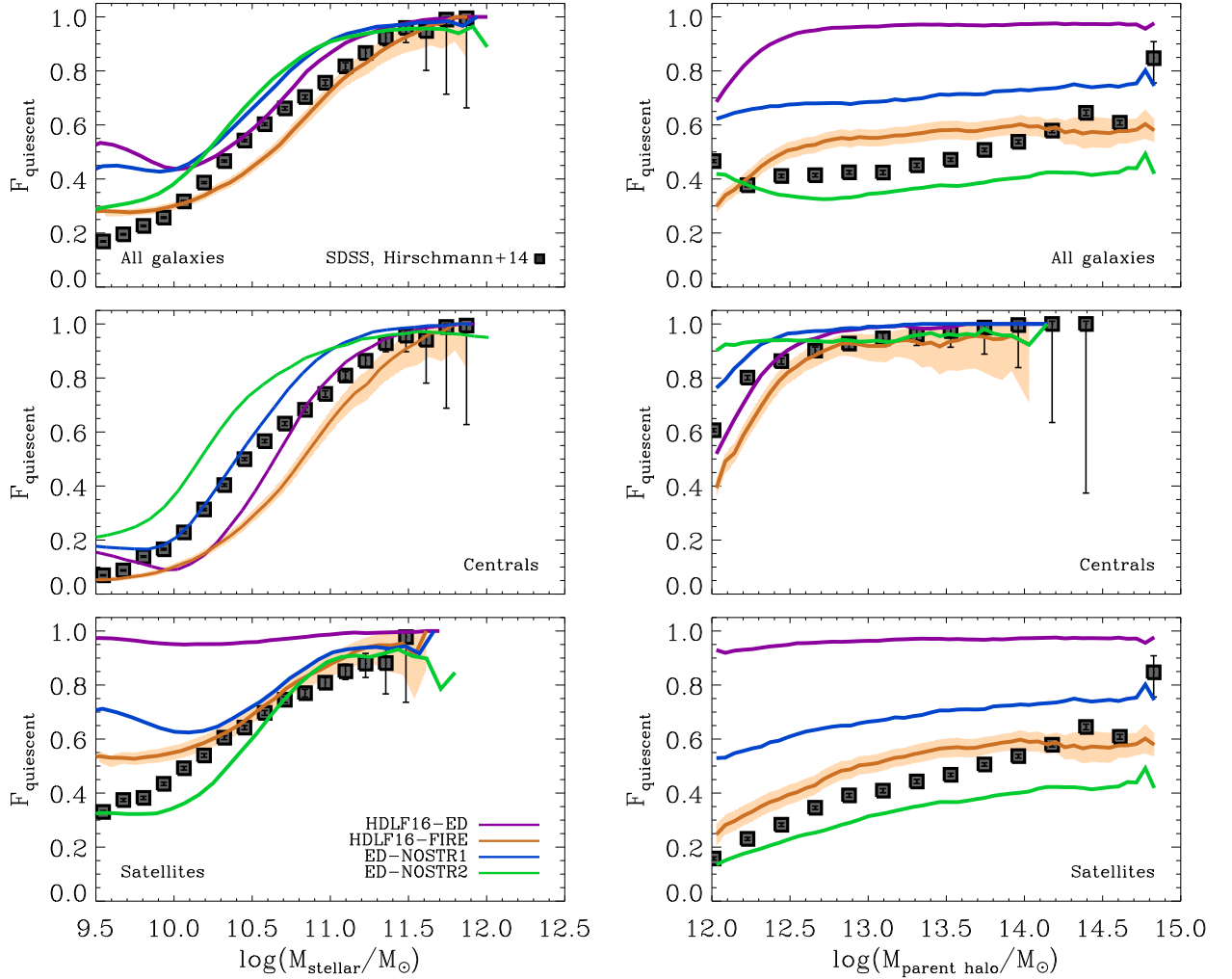


Figure 2. Present-day quiescent fraction of all galaxies (top row), centrals (middle row), and satellites (bottom row) as a function galaxy stellar mass (left column) and halo mass (right column). Filled symbols with error bars correspond to observational measurements based on the SDSS (Hirschmann et al. 2014). Lines of different colours correspond to the different runs used in this study.

tom). The top panels show that the HDLF16-FIRE model reproduces approximately well the measured variations of passive fractions both as a function of galaxy stellar mass and as a function of halo mass. At intermediate galaxy mass and halo masses, model predictions are slightly below and above the observed values, respectively. For the lowest galaxy stellar masses considered, our fiducial model tends to over-predict passive fractions. This could be probably alleviated by removing the assumption of instantaneous hot gas stripping and by including an explicit treatment for gas/stellar stripping. All other runs considered over-predict the fractions of passive galaxies for galaxy masses below $\sim 10^{10} M_{\odot}$. As expected, the largest excess is found for the HDLF16-ED run, that also significantly over-predicts the fraction of passive galaxies measured as a function of halo mass, for the entire mass range considered. Assuming cooling can continue on satellite galaxies that retain their parent dark matter substructure (ED-NOSTR1) improves the agreement with observational measurements, but does not resolve the excess of low-mass passive galaxies. Only by making the unrealis-

tic assumption that gas cooling can still continue on orphan galaxies until the hot gas is exhausted (this is the case in the ED-NOSTR2 run), are we able to significantly reduce the fraction of passive galaxies predicted at low masses. In this run, the predicted passive fraction as a function of halo mass is even lower than measured in the data, particularly for the most massive haloes.

The middle panels of Fig. 2 show the fraction of passive central galaxies, as predicted and estimated from data. For virtually all galaxy stellar masses considered, with the exception of the most massive galaxies, our fiducial HDLF16-FIRE model under-predicts the measured fraction of passive centrals, while the ED-NOSTR2 tends to over-predict it. The reason for this is that, in this run, less hot gas is able to cool onto central galaxies because a certain fraction of it remains associated with infalling satellites and contributes to replenish their cold gas reservoir. The over-prediction of passive centrals in this run is such that there is no significant variation of the central passive fraction as a function of halo mass (middle right panel). The other runs perform some-

what better, with the HDLF16-FIRE model under-predicting the fraction of passive central galaxies for haloes less massive than $\sim 10^{12.5} M_{\odot}$.

The bottom panels of Fig. 2 show the fraction of passive satellite galaxies, as predicted from all runs considered and as measured from data. The figure clearly shows that virtually all satellites in the HDLF16-ED run are passive, with very little trend as a function of galaxy stellar mass. The run also over-predicts by large factors the measured fraction of passive satellites as a function of halo mass (bottom right panel). Relaxing the approximation of instantaneous hot gas stripping reduces the overall fraction of passive satellites and introduces a trend as a function of galaxy mass. For the lowest galaxy masses considered, the observed passive fraction can only be reproduced, in the framework of the HDLF16-ED feedback scheme, assuming that gas can cool also on orphan galaxies at the rate predicted considering halo properties at the time of satellite accretion. The same run, however, under-predicts the fraction of passive satellites for all haloes more massive than $\sim 10^{13} M_{\odot}$. The HDLF16-FIRE model is in good agreement with observational data for galaxies more massive than $\sim 10^{10.3} M_{\odot}$, while it still over-predicts the fraction of passive satellites for lower galaxy masses. This indicates the necessity and importance to improve the adopted treatment for satellite galaxies at low masses. This could likely also improve the agreement with the measured fractions of passive satellites as a function of halo mass.

Results shown in Fig. 2 do not depend on the resolution of the simulation, but for the ED-NOSTR1 model (see Appendix A). In this case, a higher resolution allows gas cooling to take place on satellites for longer times (down to lower substructure masses), which makes the passive satellite fractions lower (closer to those predicted by the ED-NOSTR2 model) at low stellar masses.

In summary, in the framework of the HDLF16-ED feedback scheme, the observed variations of passive fractions as a function of galaxy stellar mass and halo mass can be reproduced, albeit not perfectly, assuming that the hot gas reservoir is retained by infalling satellites, and that gas cooling can take place on them until the hot reservoir is completely exhausted. A comparable level of agreement with data can be obtained also by assuming a different feedback scheme, albeit still adopting an instantaneous stripping of the hot gas reservoir (as in the HDLF16-FIRE run). Since the assumptions adopted in the former approach are unrealistic, and it does not reproduce the observed evolution of the galaxy stellar mass function, we favour the HDLF16-FIRE model as a better solution to the ‘over-quenching’ problem discussed earlier. The agreement with data is not perfect in neither cases, but our exercise demonstrates that the observed variations of passive fractions are not exclusively determined by environmental effects and can, in fact, be significantly affected by a modified treatment of stellar feedback.

Finally, we note that a more accurate comparison between model predictions and observational data would require running the same group finder employed for the observations on our model catalogues. In fact, [Campbell et al. \(2015\)](#) have shown that correlated scatter in galaxy colour at fixed central luminosity and central/satellite misidentification affect the colour-dependent halo occupation statistics. While this has an impact on the detailed comparison between observations and model predictions (particularly for

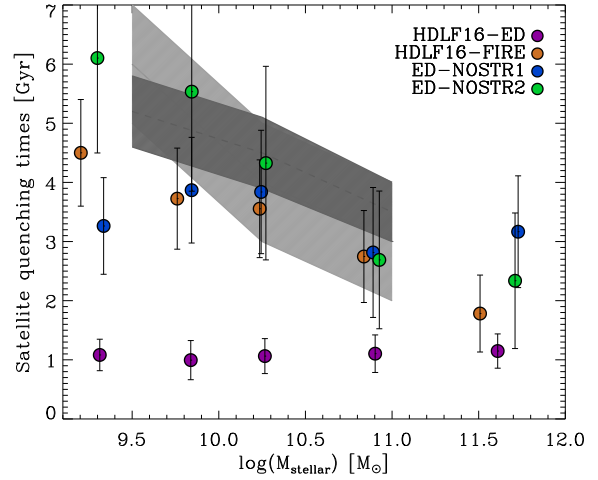


Figure 3. Satellite quenching time-scales versus galaxy stellar mass. The grey shaded regions represent observational estimates by [Wetzel et al. \(2013\)](#), dark grey) and [Hirschmann et al. \(2014\)](#), light grey). Symbols of different colour show model predictions from the four runs considered in this study, as indicated in the legend. Only model satellites that are passive at present and that were star forming at infall (see text for detail) have been considered. For model predictions, we show the mean values of the quenching time-scales and their scatter.

central galaxies), it does not significantly affect our conclusions.

4 QUENCHING TIME-SCALES

In addition to passive fractions and their trends as a function of galaxy mass and halo mass, it is also interesting to evaluate the time-scales over which the star formation in satellite model galaxies is suppressed, and compare model predictions with available observational estimates. In this section, we use the ‘quenching time-scales’ estimated by [Wetzel et al. \(2013\)](#) and the ‘refined’ estimates by [Hirschmann et al. \(2014\)](#). As mentioned in Section 1, these are obtained combining observational estimates of the variation of passive fractions and of the specific SFR distributions with either infall histories extracted from N-body simulations or galaxy merger trees extracted from semi-analytic models. In [Hirschmann et al. \(2014\)](#), we demonstrated that the ‘refined’ estimates are consistent with those obtained considering the time elapsed between the last time each model galaxy was central and star forming, and the first time it became a satellite passive galaxy. In addition, for this calculation, we only consider present-day passive satellites that are star-forming at the time of infall (i.e. were not already quenched before accretion).

Fig. 3 shows how model predictions from the runs considered here (circles of different colours) compare to observational estimates. The quenching time-scales predicted by our HDLF16-ED feedback schemes are very short, of the order of ~ 1 Gyr, and do not depend on galaxy stellar mass. Longer time-scales can be obtained both by relaxing the assumption of instantaneous hot gas stripping and by modifying the adopted stellar feedback scheme. The strongest

trend as a function of galaxy stellar mass is obtained for the ED-NOSTR2 model, that predicts quenching time-scales as long as ~ 6 Gyrs for galaxies with stellar mass $\sim 9.8 M_{\odot}$. For galaxies of the same mass, our HDLF16-FIRE model predicts quenching time-scales that are somewhat lower but still within the uncertainties of the observational estimates. For the most massive galaxies, where observational estimates are not available, predictions from the HDLF16-FIRE run are consistent with those from the HDLF16-ED run, and are lower than those predicted by the other model variants considered. The figure confirms that the evolution of satellite galaxies can be influenced by both internal physical processes (stellar feedback in this case) and by environmental processes. Our model does not include the effect of ram-pressure stripping of cold gas and/or tidal stellar stripping. We expect, however, these processes to be more important in more massive systems and therefore not for the bulk of the satellite population from the observational samples considered.

5 DISCUSSION

In the previous sections, we have shown that our fiducial HDLF16-FIRE model is able to reproduce relatively well (albeit not perfectly) the variations of passive fractions measured in the nearby Universe, as well as the relatively long quenching time-scales inferred from data. This is somewhat surprising as our fiducial feedback scheme assumes instantaneous stripping of the hot gas associated with infalling satellites. Below (in Section 5.1), we explain in detail how the better agreement with data is achieved. We have shown that a relatively good agreement with data can be also found relaxing the assumption of instantaneous hot gas stripping at infall. In this case, however, it is necessary to assume that gas cooling continues until exhaustion of the hot gas reservoir, at a rate predicted considering halo properties at the time of satellite infall, even after the hosting dark matter substructure has been stripped below the resolution limit of the simulation. One obvious question is if the same level of agreement is maintained in both runs at higher redshift and/or if higher redshift data can be used to discriminate among alternatives models. We will address this question below (Section 5.2).

5.1 The success of our fiducial HDLF16-FIRE feedback scheme

The top panels of Fig. 4 show the gas fractions at the time of infall for galaxies that are passive satellites today and were star forming at the time of infall, in different bins of galaxy stellar mass (different columns, as indicated by the legend). There is a clear offset between the HDLF16-FIRE and HDLF16-ED schemes, with the former predicting systematically higher gas fractions than the latter, for all galaxy masses and independently of the infall time. The figure also shows that the predicted gas fractions increase with decreasing galaxy stellar mass, in qualitative agreement with observational measurements (for a quantitative comparison with data, see Fig. 5 in Hirschmann et al. 2016). When relaxing the assumption of instantaneous hot gas stripping, the gas fractions at infall generally increase with respect to predictions from the HDLF16-ED run, as expected. The

increase is modest or negligible for the most massive galaxies, but becomes more significant at lower galaxy masses: in the ED-NOSTR2 run, satellites of mass $\sim 10^9 M_{\odot}$ accreted earlier than ~ 8 Gyr ago have gas fractions that are even *larger* than in the HDLF16-FIRE run. In addition, the two runs assuming non-instantaneous hot gas stripping predict a stronger dependence of the cold gas fraction on infall time with respect to our fiducial and HDLF16-ED runs. Thus, in principle, measurements of gas fractions as a function of cosmic time could be used to discriminate between the different runs used here. In practice, however, the scatter in predicted gas fraction at fixed galaxy stellar mass is typically rather large, and observational measurements also carry large uncertainties.

The middle panels of Fig. 4 show the evolution of the cold gas mass associated with galaxies that are passive satellites today, and that were accreted between 6 and 7 Gyrs ago. These average trends have been obtained by linking each model galaxy to its most massive progenitor at each previous cosmic epoch, and have been rescaled to the time of accretion (i.e. the last time the galaxy was central). We have verified that the trends remain the same for earlier/later accretion times, but the relative importance of external/internal processes varies. The cold gas mass increases at early times due to cosmological infall, and later decreases due to a combination of star formation and stellar feedback dominating over gas cooling. For galaxies with stellar mass larger than $\sim 10^{11} M_{\odot}$, the decrease of cold gas, due to star formation, starts before galaxies become satellites. At fixed galaxy mass today, the cold gas mass at accretion is largest in the HDLF16-FIRE run and lowest for the ED-NOSTR2 run. After accretion, the replenishment of new cold gas via cooling is suppressed in the HDLF16-FIRE and HDLF16-ED runs, and delayed gas recycling from previous stellar populations does not contribute significant amounts of cold gas. As a consequence, cold gas always decreases after accretion due to a combination of star formation and stellar feedback. The decrease is more rapid in the HDLF16-ED model due to a higher rate of reheating (see Fig. 4 in Hirschmann et al. 2016). In the ED-NOSTR1 and ED-NOSTR2 runs, gas cooling can continue after accretion until the galaxy becomes orphan in the former run, or until hot gas is exhausted in the latter. For galaxies of low to intermediate stellar mass, this is enough to prevent a significant decrease of the cold gas mass for relatively long times. For more massive galaxies, that have lower gas fractions at the time of accretion (see top panels), the evolution predicted in these two runs is instead closer to that predicted by the HDLF16-ED model. Among the four runs considered, the HDLF16-FIRE exhibits the most rapid increase of cold gas before accretion, and the slowest depletion at later times.

The bottom panels of Fig. 4 show the distribution of accretion times for the same satellite galaxies considered in the top panels. Satellites have been accreted over a range of cosmic epochs, with the most massive galaxies being accreted on average later than lower mass galaxies (this is a natural consequence of hierarchical accretion; De Lucia et al. 2012). Interestingly, we find that galaxies selected in fixed bins of stellar mass at $z=0$ correspond to different median accretion times. In particular, galaxies in the HDLF16-FIRE exhibit the distributions that are most skewed towards later cosmic times. Therefore, on average, present day passive satellites in

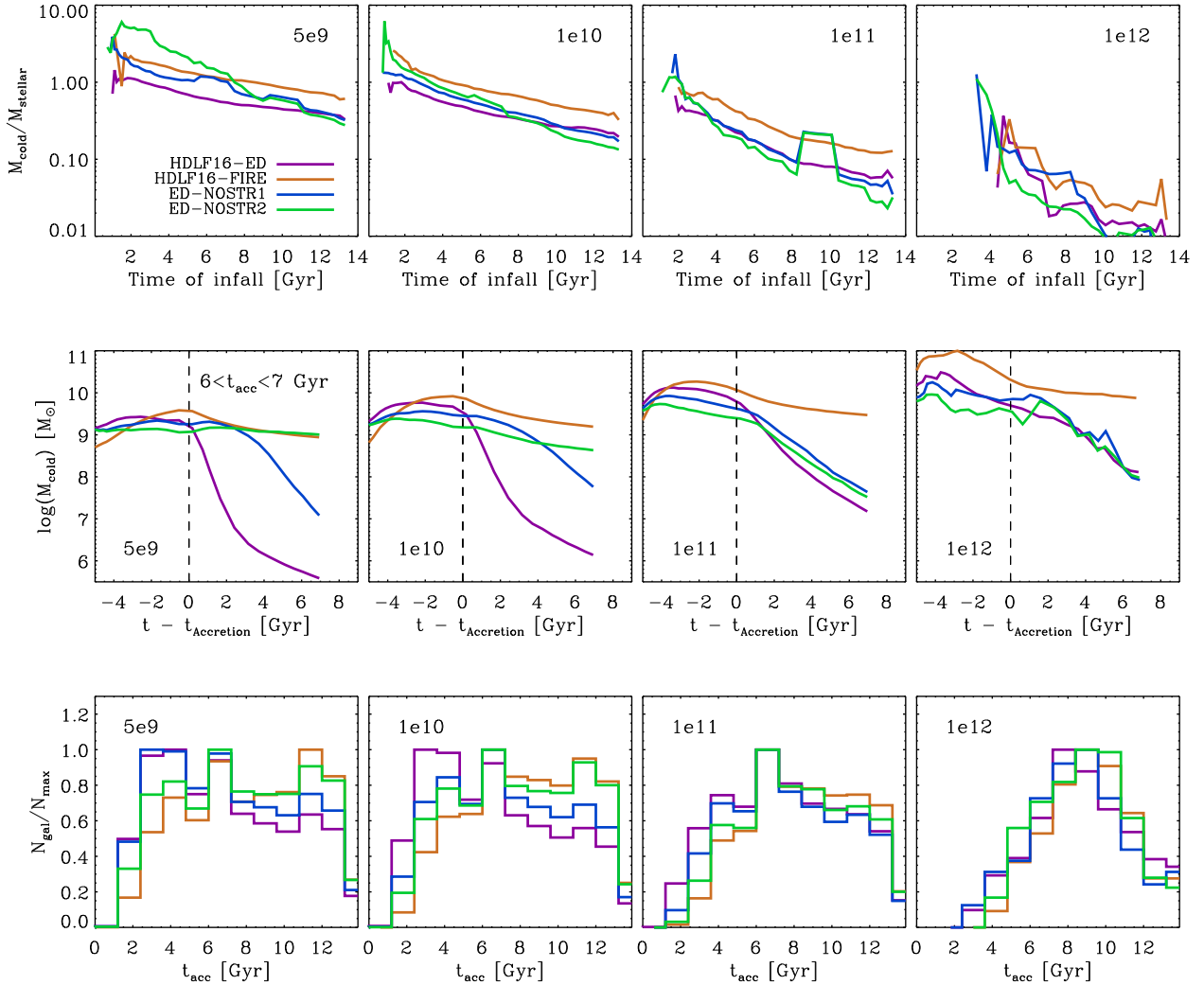


Figure 4. Top row: cold gas fractions at the time of infall for galaxies that are passive satellites at $z=0$ and that were star forming at the time of infall. Middle row: evolution (rescaled to the time of accretion) of the cold gas mass associated with present day passive satellites that were accreted between 6 and 7 Gyrs ago. Bottom row: distribution of the accretion times of the same satellites considered for the top panels. Different columns correspond to different galaxy stellar mass bins at $z = 0$, as indicated in the legend.

this run have suffered environmental processes for a shorter time than satellites of the same mass in the other runs. It is worth noting, however, that gas fractions tend to decrease with cosmic time, and that the range of accretion times is very large at all stellar masses and in all runs considered in this study.

In summary, the better agreement with data of our HDLF16-FIRE run with respect to predictions from the HDLF16-ED run is due to the fact that (i) galaxies are generally more gas-rich (and therefore more star forming) at infall, and (ii) the gas re-heating rate assumed in the HDLF16-FIRE run is lower than that adopted in the HDLF16-ED run, allowing satellites to keep their star-forming reservoir for longer times.

5.2 Passive fractions and quenching time-scales at higher redshift

The analysis presented in the previous sections is focused on the local Universe, where detailed measurements of the variations of passive fractions as a function of galaxy stellar mass and halo mass (or alternative definitions of the environment) are available. At higher redshifts, statistical studies are more difficult, due to the more limited availability of spectroscopic redshifts and overall less accurate measurements of the star formation activity. The situation is rapidly improving, and will be revolutionized in the next future with the advent of new space missions like the James Webb Space Telescope and Euclid and highly multiplexed spectroscopic instruments from the ground (e.g., MOONS at VLT).

Being a regime that has not been used to tune our model parameters, the high redshift can potentially discriminate among alternative scenarios. While we defer to a future study an accurate comparison between model predic-

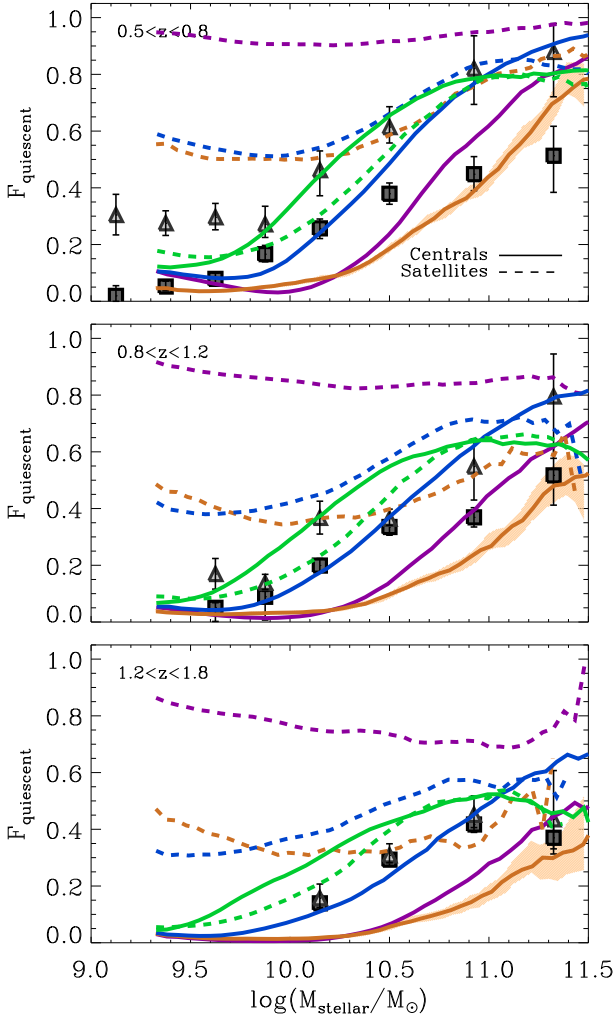


Figure 5. Fraction of passive centrals and satellite galaxies at $0.5 < z < 1.8$. Lines of different colours correspond to the different model runs considered in this study (solid and dashed are used for centrals and satellites, respectively). Symbols with error bars (squares and triangles are for centrals and satellites, respectively) correspond to observational estimates by Fossati et al. (2017).

tions and different observational measurements of the passive/quenched fraction in different environment, we present in this section a preliminary comparison with measurements by Fossati et al. (2017). These authors have used spectroscopic and grism redshifts in the five CANDELS/3D-HST fields (Grogin et al. 2011; Koekemoer et al. 2011; Brammer et al. 2012) to characterize the environment of galaxies in the redshift range $0.5 < z < 3.0$. Multi-wavelength photometry has been used to classify galaxies as ‘passive’, and the fractions of passive centrals and satellites have been evaluated as a function of stellar mass to quantify, using the same approach used for low- z data, the fraction of galaxies whose star formation activity was suppressed by environment specific processes. In Fig. 5, we show how observational estimates for central (squares) and satellite (triangles) galaxies compare to predictions from the different runs considered above (solid and dashed lines are used for centrals

and satellites, respectively). Model galaxies are classified as passive according to their specific SFR (see Section 3), while a colour-colour selection has been employed for the observational data. We have verified, however, that results are qualitatively the same when using for model galaxies the same colour selection adopted in Fossati et al. Results in Fig. 5 show that the fraction of passive galaxies tend to decrease at increasing redshift, both in the models and in the data. None of the models considered, however, reproduce well the observed trends: the HDLF16-ED run over-predicts significantly the fraction of passive satellites at all redshifts considered. The passive fractions of satellites are lower in the other runs, and the predictions from the HDLF16-FIRE model appear to be in relatively good agreement with observational estimates for the most massive satellites ($> 10^{10} M_{\odot}$). For central galaxies, the variation of passive fractions as a function of galaxy stellar mass is stronger than observed in all runs considered. At the massive end, observational data appear to be closer to predictions from the HDLF16-FIRE run, while for galaxies below $\sim 10^{10} M_{\odot}$, data are close to the predictions from the ED-NOSTR1 model. For all redshift bins considered, the difference between passive fractions for centrals and satellites remain large in all model runs considered, while it decreases significantly in the data: at the highest redshift the measurements for passive and centrals are very similar.

As done in the previous section, we have also estimated the quenching time-scales for passive satellite galaxies at different redshifts, and compared our model predictions with observational estimates by Fossati et al. (2017). As said above, these are obtained using the same approach adopted for the SDSS data. Results are shown in Fig. 6. Both the inferred and predicted quenching time-scales decrease at earlier cosmic epochs, but the decrease is larger for the theoretical predictions. At $z = 0.5$, data suggest a still relatively strong trend as a function of galaxy stellar mass. This is found also in the HDLF16-FIRE run and in the runs assuming a non-instantaneous stripping of the hot gas. The differences between these three runs are smaller than at $z = 0$, and the predicted quenching time-scales are lower than those inferred from the data for galaxies with stellar mass $< 10^{10.5} M_{\odot}$. At higher redshifts, model predictions get even closer, with predicted quenching time-scales of the order of 1 Gyr for galaxies of all masses at $z = 1.5$. While the trend as a function of galaxy stellar mass becomes less significant with increasing redshift also in the data, the inferred quenching time-scales are more than a factor ~ 2 larger than model predictions at $z = 1.5$. As shown above and in the previous section, the HDLF16-FIRE model over-predicts the fraction of passive satellites at low masses, and the disagreement becomes more important with increasing redshift. A treatment of the non-instantaneous stripping of the hot gas within our reference stellar feedback model can improve the agreement with data over this mass range. We will address this in future work, where we will also consider an explicit treatment for cold gas removal by ram-pressure, and will carry out a more detailed comparison with observational measurements at high redshift in different environments (e.g. Balogh et al. 2016; Cucciati et al. 2017; Kawinwanichakij et al. 2017; Guo et al. 2017).

6 CONCLUSIONS

We have used our state-of-the-art Galaxy Evolution and Assembly (GAEA) semi-analytic model to analyse the characteristic time-scales of star formation and gas consumption in satellite galaxies. In previous work, we have shown that our fiducial model (HDLF16-FIRE in this study) is able to reproduce the measured evolution of the galaxy stellar mass function and cosmic SFR over a significant fraction of the cosmic time (Hirschmann et al. 2016; Fontanot et al. 2017). In addition, it exhibits a very good agreement with important scaling relations like the mass-metallicity relation and its evolution as a function of cosmic time (Hirschmann et al. 2016; Xie et al. 2017). In this study, we have shown that our fiducial model also reproduces reasonably well the variations of passive fractions as a function of galaxy stellar mass and halo mass measured in the local Universe, as well as the long quenching time-scales that are inferred from data.

The same level of agreement can be obtained by using an alternative stellar feedback scheme, that has been employed in previous versions of our model (HDLF16-ED) and modifying the treatment adopted for satellite galaxies. We find that a good agreement with the passive fractions measured in the local Universe can be obtained only by making the unrealistic assumption that cooling can continue on satellite galaxies, at the rate predicted using halo properties at the time of satellite infall, even after their parent dark matter substructures have been stripped below the resolution limit of the simulation, and until complete exhaustion of the hot gas (ED-NOSTR2). The stellar feedback scheme adopted in this case, however, leads to a significant over-production of low-to-intermediate mass galaxies in our GAEA framework.

We demonstrate that the better agreement of the HDLF16-FIRE model with respect to previous versions of our semi-analytic model can be ascribed to (i) a larger cold gas fraction of satellites at the time of accretion and (ii) a reheating rate that is lower than in our older stellar feedback scheme. These elements keep satellite galaxies active for time-scales that are significantly longer than in previous versions of our model. A preliminary comparison with observational estimates at higher redshift shows that our HDLF16-FIRE model reproduces well the observed passive fractions of satellites with stellar mass larger than $\sim 10^{10} M_{\odot}$, but tends to over-predict the passive satellite fractions for lower mass galaxies and under-predict the fraction of passive centrals.

Our results highlight the need to improve the adopted treatment for satellites at low-mass in our HDLF16-FIRE model. Given the overall better agreement of our reference stellar feedback scheme, we argue that this is important only for galaxy stellar masses below $\sim 10^{10} M_{\odot}$. For more massive galaxies, the abundance of passive fractions is determined primarily by the self-regulation between star formation and stellar feedback, and is only marginally affected by environmental processes. In future work, we plan to include an explicit treatment for non-instantaneous stripping and for cold gas removal by ram-pressure, and to carry out a more detailed comparison with observational measurements at earlier cosmic epochs.

ACKNOWLEDGEMENTS

We thank Matteo Fossati for his providing observational estimates in electronic form, and for useful comments on a preliminary version of this paper. GDL acknowledges financial support from the MERAC foundation. MH acknowledges financial support from the European Research Council via an Advanced Grant under grant agreement no. 321323 NEO-GAL.

REFERENCES

- Bahé Y. M., et al., 2017, *MNRAS*, **470**, 4186
 Baldry I. K., Balogh M. L., Bower R. G., Glazebrook K., Nichol R. C., Bamford S. P., Budavari T., 2006, *MNRAS*, **373**, 469
 Balogh M., et al., 2004, *MNRAS*, **348**, 1355
 Balogh M. L., et al., 2016, *MNRAS*, **456**, 4364
 Boylan-Kolchin M., Springel V., White S. D. M., Jenkins A., Lemson G., 2009, *MNRAS*, **398**, 1150
 Brammer G. B., et al., 2012, *ApJS*, **200**, 13
 Brinchmann J., Charlot S., White S. D. M., Tremonti C., Kauffmann G., Heckman T., Brinkmann J., 2004, *MNRAS*, **351**, 1151
 Campbell D., van den Bosch F. C., Hearin A., Padmanabhan N., Berlind A., Mo H. J., Tinker J., Yang X., 2015, *MNRAS*, **452**, 444
 Cooper M. C., et al., 2012, *MNRAS*, **419**, 3018
 Croton D. J., 2006, *MNRAS*, **369**, 1808
 Cucciati O., et al., 2017, *A&A*, **602**, A15
 De Lucia G., Blaizot J., 2007, *MNRAS*, **375**, 2
 De Lucia G., Kauffmann G., White S. D. M., 2004, *MNRAS*, **349**, 1101
 De Lucia G., Boylan-Kolchin M., Benson A. J., Fontanot F., Monaco P., 2010, *MNRAS*, **406**, 1533
 De Lucia G., Weinmann S., Poggianti B. M., Aragón-Salamanca A., Zaritsky D., 2012, *MNRAS*, **423**, 1277
 De Lucia G., Muzzin A., Weinmann S., 2014a, *New Astron. Rev.*, **62**, 1
 De Lucia G., Tornatore L., Frenk C. S., Helmi A., Navarro J. F., White S. D. M., 2014b, *MNRAS*, **445**, 970
 Dressler A., 1980, *ApJ*, **236**, 351
 Farouki R., Shapiro S. L., 1981, *ApJ*, **243**, 32
 Fillingham S. P., Cooper M. C., Wheeler C., Garrison-Kimmel S., Boylan-Kolchin M., Bullock J. S., 2015, *MNRAS*, **454**, 2039
 Fillingham S. P., Cooper M. C., Pace A. B., Boylan-Kolchin M., Bullock J. S., Garrison-Kimmel S., Wheeler C., 2016, *MNRAS*, **463**, 1916
 Font A. S., et al., 2008, *MNRAS*, **389**, 1619
 Fontanot F., Hirschmann M., De Lucia G., 2017, *ApJ*, **842**, L14
 Fossati M., et al., 2017, *ApJ*, **835**, 153
 Franx M., van Dokkum P. G., Schreiber N. M. F., Wuyts S., Labbé I., Toft S., 2008, *ApJ*, **688**, 770
 Giovanelli R., Haynes M. P., 1983, *AJ*, **88**, 881
 Grogin N. A., et al., 2011, *ApJS*, **197**, 35
 Gunn J. E., Gott III J. R., 1972, *ApJ*, **176**, 1
 Guo Q., et al., 2011, *MNRAS*, pp 164+
 Guo Q., White S., Angulo R. E., Henriques B., Lemson G., Boylan-Kolchin M., Thomas P., Short C., 2013, *MNRAS*, **428**, 1351
 Guo Y., et al., 2017, *ApJ*, **841**, L22
 Henriques B. M. B., White S. D. M., Thomas P. A., Angulo R. E., Guo Q., Lemson G., Springel V., 2013, *MNRAS*, **431**, 3373
 Henriques B. M. B., White S. D. M., Thomas P. A., Angulo R. E., Guo Q., Lemson G., Wang W., 2017, *MNRAS*, **469**, 2626
 Hirschmann M., De Lucia G., Wilman D., Weinmann S., Iovino A., Cucciati O., Zibetti S., Villalobos Á., 2014, *MNRAS*, **444**, 2938

- Hirschmann M., De Lucia G., Fontanot F., 2016, *MNRAS*, **461**, 1760
- Hopkins P. F., Kereš D., Oñorbe J., Faucher-Giguère C.-A., Quataert E., Murray N., Bullock J. S., 2014, *MNRAS*, **445**, 581
- Kang X., van den Bosch F. C., 2008, *ApJ*, **676**, L101
- Kauffmann G., White S. D. M., Heckman T. M., Ménard B., Brinchmann J., Charlot S., Tremonti C., Brinkmann J., 2004, *MNRAS*, **353**, 713
- Kawinwanichakij L., et al., 2017, *ApJ*, **847**, 134
- Kimm T., et al., 2009, *MNRAS*, **394**, 1131
- Koekemoer A. M., et al., 2011, *ApJS*, **197**, 36
- McCarthy I. G., Frenk C. S., Font A. S., Lacey C. G., Bower R. G., Mitchell N. L., Balogh M. L., Theuns T., 2008, *MNRAS*, **383**, 593
- Mihos J. C., 2004, Clusters of Galaxies: Probes of Cosmological Structure and Galaxy Evolution, **p. 277**
- Moore B., Katz N., Lake G., Dressler A., Oemler A., 1996, *Nature*, **379**, 613
- Muratov A. L., Kereš D., Faucher-Giguère C.-A., Hopkins P. F., Quataert E., Murray N., 2015, *MNRAS*, **454**, 2691
- Oemler Jr. A., 1974, *ApJ*, **194**, 1
- Peng Y.-j., et al., 2010, *ApJ*, **721**, 193
- Pillepich A., et al., 2018, *MNRAS*, **473**, 4077
- Sales L. V., et al., 2015, *MNRAS*, **447**, L6
- Salim S. e. a., 2007, *ApJS*, **173**, 267
- Springel V., et al., 2005, *Nature*, **435**, 629
- Wang L., Li C., Kauffmann G., De Lucia G., 2007, *MNRAS*, **377**, 1419
- Wang J., De Lucia G., Kitzbichler M. G., White S. D. M., 2008, *MNRAS*, **384**, 1301
- Weinmann S. M., van den Bosch F. C., Yang X., Mo H. J., 2006a, *MNRAS*, **366**, 2
- Weinmann S. M., van den Bosch F. C., Yang X., Mo H. J., Croton D. J., Moore B., 2006b, *MNRAS*, **372**, 1161
- Weinmann S. M., Kauffmann G., von der Linden A., De Lucia G., 2010, *MNRAS*, **406**, 2249
- Weinmann S. M., Pasquali A., Oppenheimer B. D., Finlator K., Mendel J. T., Crain R. A., Macciò A. V., 2012, *MNRAS*, **426**, 2797
- Wetzel A. R., Tinker J. L., Conroy C., 2012, *MNRAS*, **424**, 232
- Wetzel A. R., Tinker J. L., Conroy C., van den Bosch F. C., 2013, *MNRAS*, **432**, 336
- Xie L., De Lucia G., Hirschmann M., Fontanot F., Zoldan A., 2017, *MNRAS*, **469**, 968
- Yang X., Mo H. J., van den Bosch F. C., Pasquali A., Li C., Barden M., 2007, *ApJ*, **671**, 153
- Zoldan A., De Lucia G., Xie L., Fontanot F., Hirschmann M., 2017, *MNRAS*, **465**, 2236
- Zoldan A., De Lucia G., Xie L., Fontanot F., Hirschmann M., 2018, preprint, ([arXiv:1803.08056](https://arxiv.org/abs/1803.08056))

APPENDIX A: RESOLUTION EFFECTS

Fig. A1 shows the fraction of passive galaxies as a function of galaxy stellar mass (left column) and parent halo mass (right column), as predicted by all model runs considered (lines of different colours), and as estimated from data (symbols with error bars). Solid lines correspond to model predictions based on the Millennium Simulation (these are the same lines shown in Fig. 2), while dashed lines correspond to the Millennium II (Boylan-Kolchin et al. 2009). Also in this case, we have used only about 20 per cent of the entire volume of the simulation, but the results shown do not change significantly considering a larger volume. Model predictions

from the Millennium II simulation have been shown only for galaxy stellar mass bins and halo mass bins where there are at least 30 galaxies, and only galaxies brighter than -18 in the r-band have been considered (as for the observational data and for model predictions based on the Millennium). For satellite galaxies (bottom panels) model predictions are not significantly affected by resolution at the low-mass end, except for the ED-NOSTR1 model. In this run, we assume that gas can cool on satellite galaxies until there is a dark matter substructure associated with the galaxy. At the time the subhalo is stripped below the resolution of the simulation, we assume that the residual hot gas reservoir is instantaneously stripped and associated with the hot reservoir of the central galaxy. Since a higher resolution allows the substructure to be traced longer, gas cooling can continue and keep the star formation active, moving model predictions closer to those of the ED-NOSTR2 model. Although this behaviour makes predictions from one of the models used dependent on resolution at the low-mass end, it does not affect our main conclusions. Interestingly, resolution also affects model predictions for central galaxies for galaxy masses below $\sim 10^{10.5} M_{\odot}$ (middle left panel), in all runs considered in this study. Specifically, higher resolution typically translates in lower fractions of quiescent low-mass centrals. This is likely due to the fact that the higher resolution of the simulation leads to a larger number of mergers with (low-mass) gas rich galaxies, which leads to bursts of star formation. We note, however, that the difference between the two resolutions is not very large considering the scatter (dashed orange region - it is similar for the other models), and might be affected by the fact that we are sampling well only relatively low-mass haloes in the Millennium II (see middle right panel).

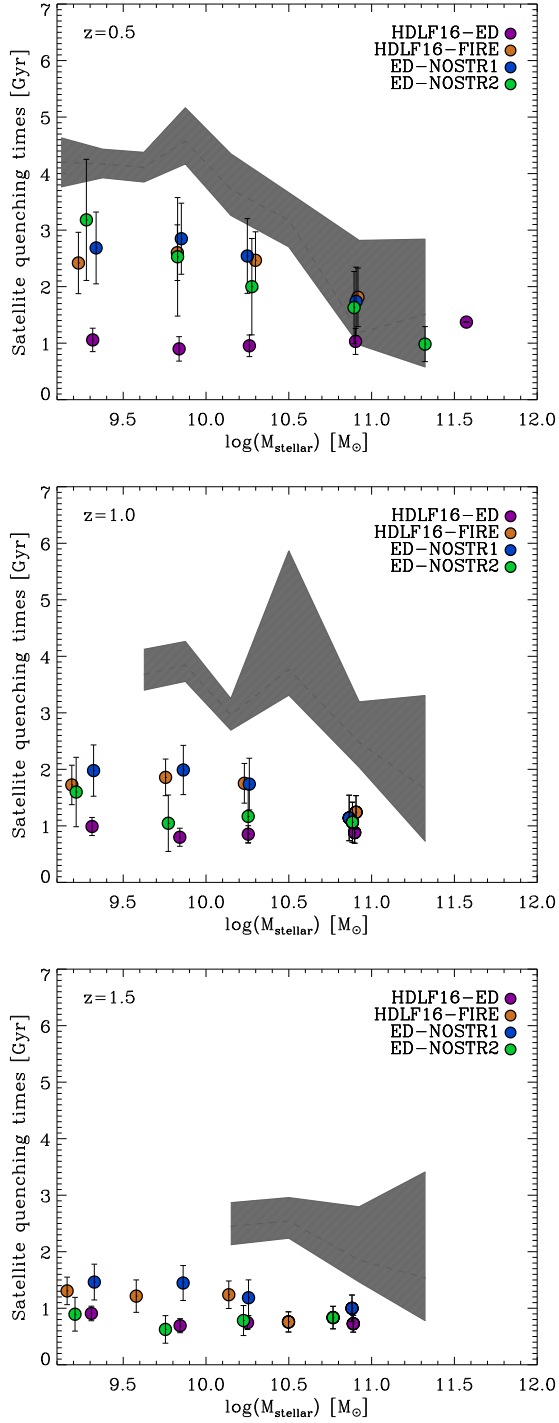


Figure 6. Quenching time-scales evaluated for passive satellites identified at different redshifts (different panels). Coloured symbols correspond to the different model runs used in this study, while dashed regions indicate observational estimates by Fossati et al. (2017).

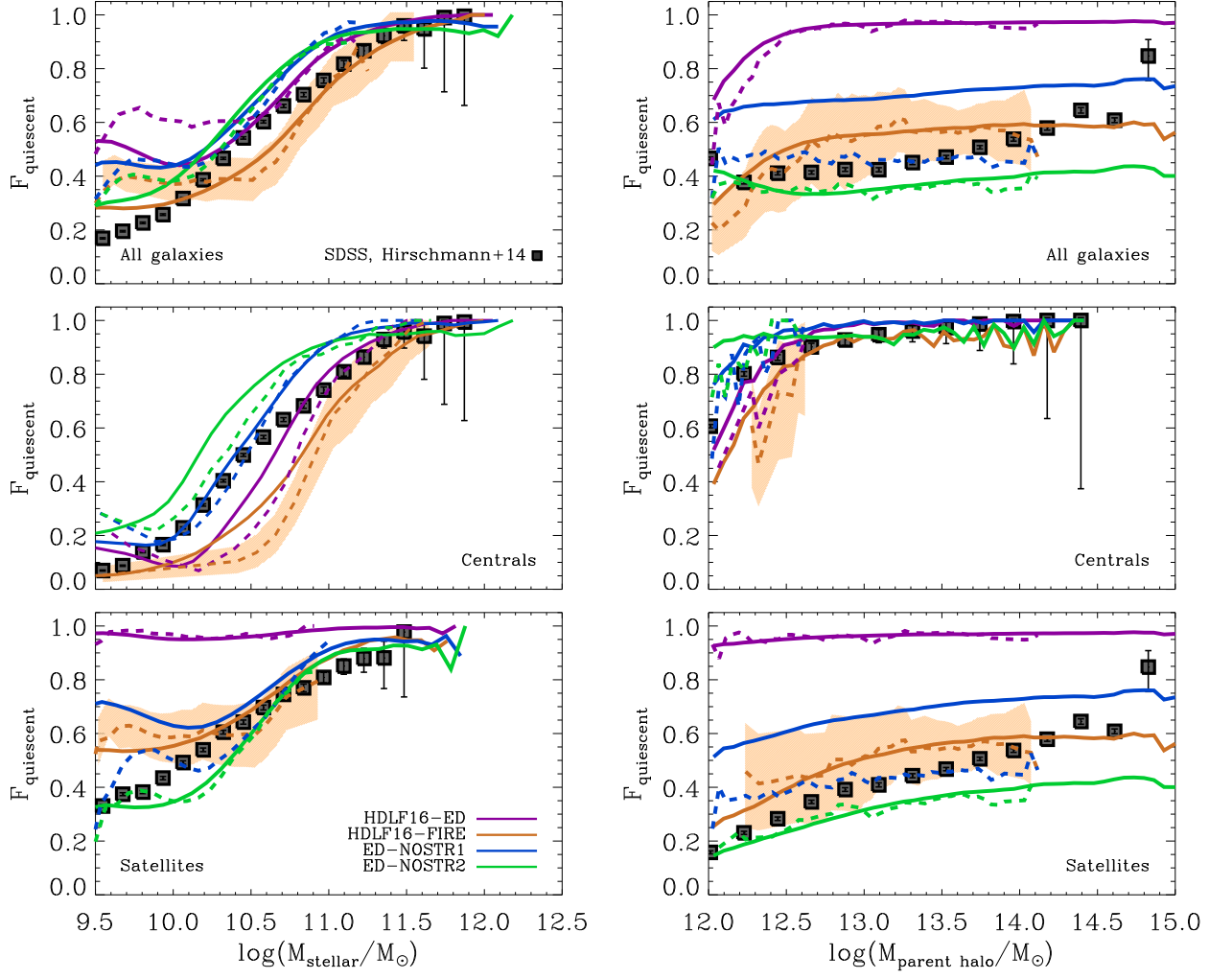


Figure A1. As Fig. 2, but including results from the MillenniumII Simulation as dashed lines.